Models for Nonheme Diiron Enzymes. Assembly of a High-Valent $Fe_2(\mu\text{-}O)_2$ Diamond Core from Its Peroxo Precursor

Yanhong Dong, Yan Zang, Lijin Shu,
Elizabeth C. Wilkinson, and Lawrence Que, Jr.*

Department of Chemistry and Center for Metals in Biocatalysis, University of Minnesota Minneapolis, Minnesota 55455

Karl Kauffmann and Eckard Münck

Department of Chemistry, Carnegie-Mellon University Pittsburgh, Pennsylvania 15213

Received September 4, 1997

High-valent intermediates have been identified in the redox cycles of the oxygen activating nonheme diiron enzymes[1] methane monooxygenase (MMO)[2] and ribonucleotide reductase (RNR).[3] For MMO, a diiron(IV) species **Q** has been observed,[4] while an iron(III)iron(IV) species **X** has been characterized for RNR.[5] Rapid-freeze-quench EXAFS studies have shown both **Q** and **X** to have Fe−Fe distances of ca. 2.5 Å.[6,7] This unusually short distance has led us to consider the possibility that these intermediates may have a bis(μ-oxo)diiron diamond core,[8] as precedented in synthetic nonheme diiron(III,IV) complexes.[9] The latter are obtained from reaction of diiron(III) complexes with H_2O_2, but no studies of the mechanism of assembly of the $Fe_2(\mu\text{-}O)_2$ diamond core have yet been reported. In this communication, we present evidence that a precursor to the bis(μ-oxo)$Fe^{III}Fe^{IV}$ complex is a (μ-oxo)(μ-1,2-peroxo)diiron(III) complex; this conversion can serve as a synthetic precedent for the formation of high-valent intermediates from their peroxo precursors in the mechanisms of RNR and MMO.

The diiron(III) complex $[Fe_2(\mu\text{-}O)_2(6\text{-}Me_3\text{-}TPA)_2](ClO_4)_2$[10] (**1**), the only crystallographically characterized example of a complex with the $Fe_2(\mu\text{-}O)_2$ diamond core, exhibits a visible spectrum is shown in Figure 1.[11] Addition of 2 equiv of H_2O_2 to **1** at −40 °C in CH_3CN generates a transient dark green species **2** that exhibits two intense absorption bands at 494 (ϵ = 1100 M^{-1} cm^{-1}) and 648 nm (ϵ = 1200 M^{-1} cm^{-1}) as well as a weak band at 846 nm (ϵ = 230 M^{-1} cm^{-1}) (Figure 1). The Mössbauer spectrum of **2** at 4.2 K displays a quadrupole doublet with ΔE_Q = 1.68(4) mm/s and δ = 0.54(2) mm/s (Figure 2A), which is distinct from the doublet reported for **1** (ΔE_Q = 1.93 mm/s and δ = 0.50 mm/s).[11] The value of δ indicates high-spin iron(III) sites, which are antiferromagnetically coupled, as indicated by the observation of an $S = 0$ ground state by studies in strong applied magnetic fields. Electrospray ionization mass spectra of **2** reveal a prominent negative ion cluster with $m/z \geq$ 1121, corresponding to $\{[Fe_2O_3(6\text{-}Me_3\text{-}TPA)_2](ClO_4)_3\}^-$, and

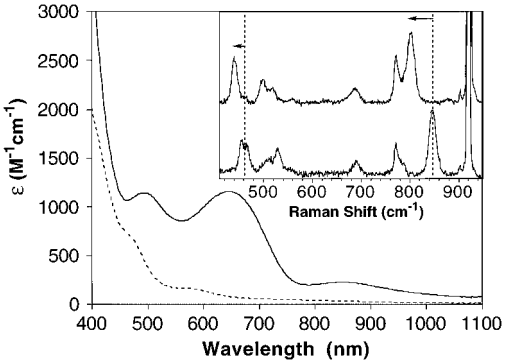

Figure 1. Visible spectra of **1** (- -) and **2** (—) in CH_3CN. Inset: Resonance Raman spectra of **2** obtained in CH_3CN using 628-nm excitation with $H_2{}^{16}O_2$ (bottom) and $H_2{}^{18}O_2$ (top).

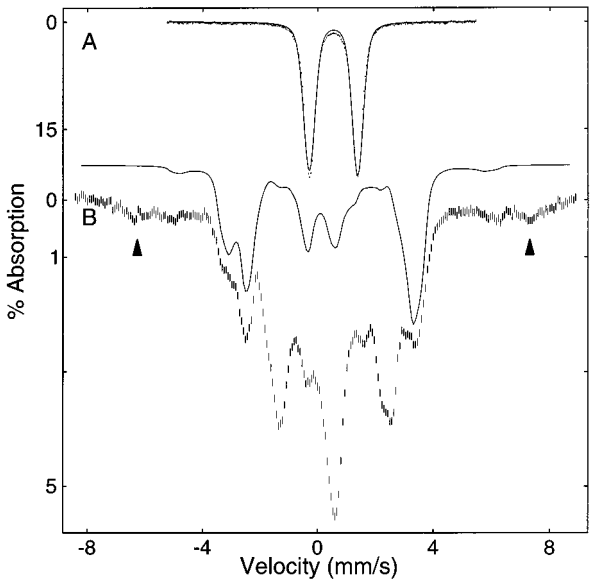

Figure 2. Mössbauer spectra of **2** (A) and its decomposition products (B). Spectra were recorded at 4.2 K in zero field (A) and in a parallel applied field of 8.0 T (B). The solid line in part A is a simulated spectrum with ΔE_Q = 1.68 mm/s and δ = 0.54 mm/s. The solid line in part B is a spectral simulation (representing 35% of Fe) outlining the contributions of the Fe(IV) and Fe(III) sites of the $S = {}^1/_2$ complex **3**; the parameters used are the same as those published for $[Fe^{III}Fe^{IV}(\mu\text{-}O)_2(6\text{-}Me\text{-}TPA)_2]^{3+}$.[9b] The triangles mark contributions of the monomeric Fe(III) species (<4% of total Fe). The three bands in the center of part B belong to the diiron(III) species. The sample in part B was frozen 25 min after addition of 1 equiv of $HClO_4$ to a 70:30 CH_3CN/C_2H_5CN solution of **2** at −30 °C.

(1) Wallar, B. J.; Lipscomb, J. D. *Chem. Rev. (Washington, D.C.)* **1996**, *96*, 2625−2657.

(2) (a) Rosenzweig, A. C.; Frederick, C. A.; Lippard, S. J.; Nordlund, P. *Nature* **1993**, *366*, 537−543. (b) Rosenzweig, A. C.; Nordlund, P.; Takahara, P. M.; Frederick, C. A.; Lippard, S. J. *Chem. Biol.* **1995**, *2*, 409−418. (c) Elango, N.; Radhakrishnan, R.; Froland, W. A.; Wallar, B. J.; Earnhart, C. A.; Lipscomb, J. D.; Ohlendorf, D. H. *Protein Sci.* **1997**, *6*, 556−568.

(3) (a) Nordlund, P.; Eklund, H. *J. Mol. Biol.* **1993**, *232*, 123−164. (b) Logan, D. T.; Su, X.-D.; Åberg, A.; Regnström, K.; Hajdu, J.; Eklund, H.; Nordlund, P. *Structure* **1996**, *4*, 1053−1064.

(4) (a) Lee, S.-K.; Nesheim, J. C.; Lipscomb, J. D. *J. Biol. Chem.* **1993**, *268*, 21569−21577. (b) Lee, S.-K.; Fox, B. G.; Froland, W. A.; Lipscomb, J. D.; Münck, E. *J. Am. Chem. Soc.* **1993**, *115*, 6450−6451. (c) Liu, K. E.; Wang, D.; Huynh, B. H.; Edmondson, D. E.; Salifoglou, A.; Lippard, S. J. *J. Am. Chem. Soc.* **1994**, *116*, 7465−7466. (d) Liu, K. E.; Valentine, A. M.; Wang, D.; Huynh, B. H.; Edmondson, D. E.; Salifoglou, A.; Lippard, S. J. *J. Am. Chem. Soc.* **1995**, *117*, 10174−10185.

(5) (a) Bollinger, J. M.; Edmondson, D. E.; Huynh, B. H.; Filley, J.; Norton, J.; Stubbe, J. *Science (Washington, D.C.)* **1991**, *253*, 292−298. (b) Ravi, N.; Bollinger, J. M.; Huynh, B. H.; Edmondson, D. E.; Stubbe, J. *J. Am. Chem. Soc.* **1994**, *116*, 8007−8014. (c) Sturgeon, B. E.; Burdi, D.; Chen, S.; Huynh, B.-H.; Edmondson, D. E.; Stubbe, J.; Hoffman, B. M. *J. Am. Chem. Soc.* **1996**, *118*, 7551−7557.

(6) Shu, L.; Nesheim, J. C.; Kauffmann, K.; Münck, E.; Lipscomb, J. D.; Que, L., Jr. *Science* **1997**, *275*, 515−518.

(7) Riggs-Gelasco, P. J.; Shu, L.; Chen, S.; Burdi, D.; Huynh, B. H.; Que, L., Jr.; Stubbe, J. *J. Am. Chem. Soc.* In press.

(8) (a) Que, L., Jr. *J. Chem. Soc., Dalton Trans.* **1997**, 3933−3940. (b) Que, L., Jr.; Dong, Y. *Acc. Chem. Res.* **1996**, *29*, 190−196.

(9) (a) Dong, Y.; Fujii, H.; Hendrich, M. P.; Leising, R. A.; Pan, G.; Randall, C. R.; Wilkinson, E. C.; Zang, Y.; Que, L., Jr.; Fox, B. G.; Kauffmann, K.; Münck, E. *J. Am. Chem. Soc.* **1995**, *117*, 2778−2792. (b) Dong, Y.; Que, L., Jr.; Kauffmann, K.; Münck, E. *J. Am. Chem. Soc.* **1995**, *117*, 11377−11378.

(10) Ligand abbreviations used: N-Et-HPTB, *N*,*N*,*N*′,*N*′-tetrakis(1-ethylbenzimidazolyl-2-methyl)-1,3-diamino-2-propanol; 6-Me-TPA, (6-methyl-2-pyridylmethyl)bis(2-pyridylmethyl)amine; 6-Me_3-TPA, tris(6-methyl-2−pyridylmethyl)amine.

(11) Zang, Y.; Dong, Y.; Que, L., Jr.; Kauffmann, K.; Münck, E. *J. Am. Chem. Soc.* **1995**, *117*, 1169−1170.

S0002-7863(97)03115-6 CCC: $14.00

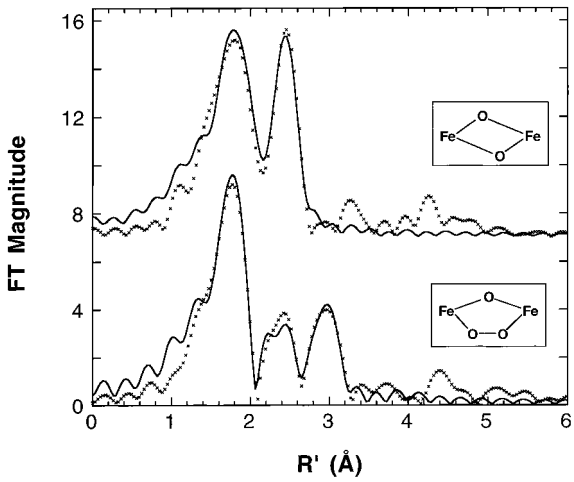

Figure 3. Fourier transforms of EXAFS data (×) and fits (—) for **1** (top, $k = 2-15$ Å^{-1}) and **2** (bottom, $k = 2-14$ Å^{-1}). Fit for **1**: 2 O at 1.86 Å, 4 N at 2.25 Å, 1 Fe at 2.67 Å, and 5 C at 2.99 Å. Fit for **2**: 2 O at 1.84 Å, 4 N at 2.23 Å, 6 C at 2.96 Å, 1 Fe at 3.14 Å, and 5 C at 3.52 Å. X-ray absorption data were collected at Beamline X9B at the National Synchrotron Light Source (NSLS).

a prominent positive ion cluster with $m/z \geq 923$, corresponding to $\{[Fe_2O_3(6\text{-}Me_3\text{-}TPA)_2](ClO_4)\}^+$. Both ions exhibit isotope intensity patterns that match the calculated ones. Moreover, upon addition of $H_2{}^{18}O$, the masses of both ion clusters increase by 2 units, consistent with the presence of an oxo bridge. Taken together, the data indicate that **2** is best formulated as $[Fe^{III}_2(O)(O_2)(6\text{-}Me_3\text{-}TPA)_2](ClO_4)_2$.

The presence of a peroxide ligand is demonstrated by the resonance Raman spectrum of **2**. Bands at 848 and 462 (Fermi doublet) cm^{-1} are observed (Figure 1 inset) which are unaffected by the presence of $H_2{}^{18}O$ but shift to 802 and 441 cm^{-1}, respectively, with the use of $H_2{}^{18}O_2$, demonstrating that they involve vibrations of the peroxide-derived oxygens. Comparison with related complexes[12] suggests that the two ^{18}O-sensitive bands can be respectively assigned to the υ_{O-O} and the υ_{Fe-O} of a bound peroxide; this assignment is consistent with the observed ^{18}O shifts of 46 and 21 cm^{-1}. Because only one quadrupole doublet is observed in the Mössbauer spectrum of **2**, it is likely that the peroxide is symmetrically coordinated to the diiron unit. The υ_{OO} of **2** is notably below the range of 880−900 cm^{-1} observed for a number of (μ-1,2-peroxo)diiron(III) complexes.[12] The weaker O−O bond observed perhaps arises from the presence of the oxo bridge in **2**; however, no suitable complex for comparison exists as **2** represents the only example of a (μ-peroxo)diiron(III) complex with an additional oxo bridge.

The core structure of **2** can be deduced by EXAFS analysis. The *R*′-space spectra of **1** and **2**, compared in Figure 3, show that the principal differences between the two species occur beyond the first coordination sphere. In fact, the first shells of both complexes can be fit with two short Fe−O bonds of ca. 1.85 Å and four longer Fe−N bonds of ca. 2.24 Å. Complex **1** exhibits an intense second sphere feature that is characteristic of an M_2O_2 diamond core structure.[9a] It derives mainly from a tightly held Fe scatterer at 2.67 Å, in good agreement with the crystallographically determined distance of 2.71 Å.[11] In contrast, **2** exhibits weaker outer shell features which indicate that the diiron core structure has been modified, with the Fe−Fe distance lengthening to 3.14 Å. When interpreted together with the other spectroscopic data, this distance suggests that **2** has a (μ-oxo)(μ-1,2-peroxo)diiron core. This conclusion is fully consistent with the dimensions of the related five-membered Fe_2O_3 ring associated with the (μ-alkoxo)(μ-1,2-peroxo)diiron core of $[Fe_2(N\text{-}Et\text{-}HPTB)(O_2)(OPPh_3)_2]^{3+}$ (r_{Fe-Fe}, 3.462(3) Å)[13] when allowing for the much shorter Fe-μ-O bonds of **2**.

Upon decomposition, **2** gives rise to a species, **3**, which exhibits an isotropic $S = {}^1/_2$ EPR signal at $g = 2.00$. This signal and the 4.2 K Mössbauer spectrum of **3** (Figure 2B) are nearly identical with those associated with $[Fe^{III}Fe^{IV}(\mu\text{-}O)_2(6\text{-}Me\text{-}TPA)_2]^{3+}$.[9b] These results suggest that **3** is the corresponding $[Fe^{III}Fe^{IV}(\mu\text{-}O)_2(6\text{-}Me_3\text{-}TPA)_2]^{3+}$ complex, a conclusion corroborated by a negative ion electrospray mass spectral cluster of peaks at $m/z \geq 1204$ with the appropriate isotope distribution pattern. Species **3** is obtained in 14% yield as estimated from the intensities of its EPR signal and Mössbauer spectrum. The yield increases to 35% (Figure 2B) when the decomposition of **2** is carried out in the presence of 1 equiv of $HClO_4$. The decay of **2** monitored at 648 nm follows pseudo-first-order kinetics with $k = 1.6 \times 10^{-3}$ s^{-1} at −30 °C and the ln [**2**] vs *t* plot remains linear over 6 half-lives. The addition of 1 equiv of $HClO_4$ accelerates the conversion of **2** to **3** by a factor of 4, thereby allowing the more efficient trapping of **3** prior to its decomposition. Thus, unlike earlier characterized diiron−peroxo complexes which break down without revealing any high-valent species,[12,13] this (μ-peroxo)diiron(III) complex decomposes to afford a metastable bis(μ-oxo)diiron(III,IV) complex.

Our observations demonstrate that an $[Fe_2(\mu\text{-}O)(\mu\text{-}O_2)]^{2+}$ intermediate is the precursor to a high-valent $[Fe_2(\mu\text{-}O)_2]^{3+}$ diamond core whose spectroscopic properties resemble those of RNR intermediate **X**.[5] This transformation may thus serve as the prototype for the formation of intermediate **X** from its putative peroxo precursor,[14] both of which require the addition of an electron to cleave the O−O bond. We have not yet identified the source of the electron in the conversion of **2** to **3**, although the excess H_2O_2 present is a likely candidate. Ongoing efforts are aimed at understanding the mechanism of this transformation. A particularly intriguing question is whether a transient diiron(IV) species may be involved; such an intermediate would also be of relevance to the mechanism of formation of intermediate **Q** in the MMO cycle from its (μ-peroxo)diiron(III) precursor.[4]

Acknowledgment. This work was supported by the National Institutes of Health (grants GM-38767 to L.Q. and GM-22701 to E.M.) and a University of Minnesota Graduate Dissertation Fellowship (to L.S.). Beamline X9B at the NSLS was supported by NIH grant RR-001633.

JA973115K

(12) (a) Dong, Y.; Ménage, S.; Brennan, B. A.; Elgren, T. E.; Jang, H. G.; Pearce, L. L.; Que, L., Jr. *J. Am. Chem. Soc.* **1993**, *115*, 1851−1859. (b) Kitajima, N.; Tamura, N.; Amagai, H.; Fukui, H.; Moro-oka, Y.; Mizutani, Y.; Kitagawa, T.; Mathur, R.; Heerwegh, K.; Reed, C. A.; Randall, C. R.; Que, L., Jr.; Tatsumi, K. *J. Am. Chem. Soc.* **1994**, *116*, 9071−9085. (c) Hayashi, Y.; Kayatani, T.; Sugimoto, H.; Suzuki, M.; Inomata, K.; Uehara, A.; Mizutani, Y.; Kitagawa, T.; Maeda, Y. *J. Am. Chem. Soc.* **1995**, *117*, 11220−11229. (d) Ookubo, T.; Sugimoto, H.; Nagayama, T.; Masuda, H.; Sato, T.; Tanaka, K.; Maeda, Y.; Okawa, H.; Hayashi, Y.; Uehara, A.; Suzuki, M. *J. Am. Chem. Soc.* **1996**, *118*, 701−702. (e) Kim, K.; Lippard, S. J. *J. Am. Chem. Soc.* **1996**, *118*, 4914−4915.

(13) Dong, Y.; Yan, S.; Young, V. G., Jr.; Que, L., Jr. *Angew. Chem., Int. Ed. Engl.* **1996**, *35*, 618−620.

(14) Tong, W. H.; Chen, S.; Lloyd, S. G.; Edmonson, D. E.; Huynh, B. H.; Stubbe, J. *J. Am. Chem. Soc.* **1996**, *118*, 2107−2108.